J|A|C|S
ARTICLES
Published on Web 11/04/2005

Intervalence Transitions in the Mixed-Valence Monocations of Bis(triarylamines) Linked with Vinylene and Phenylene−Vinylene Bridges

Stephen Barlow,*[,†,‡] Chad Risko,[†] Sung-Jae Chung,[†,‡] Neil M. Tucker,[‡] Veaceslav Coropceanu,[†] Simon C. Jones,[†] Zerubba Levi,[†] Jean-Luc Brédas,[†] and Seth R. Marder[†,‡]

Contribution from the Center for Organic Photonics and Electronics and School of Chemistry and Biochemistry, Georgia Institute of Technology, Atlanta, Georgia 30332-0400, and Department of Chemistry, University of Arizona, Tucson, Arizona 85721

Received June 22, 2005; E-mail: stephen.barlow@chemistry.gatech.edu

Abstract: (*E*)-4,4′-Bis{bis(4-methoxyphenyl)amino}stilbene, **1**, (*E*,*E*)-1,4-bis[4-{bis(4-methoxyphenyl)-amino}styryl]benzene, **2**, and two longer homologues, (*E*,*E*,*E*)-4,4′-bis[4-{bis(4-methoxyphenyl)amino}-styryl]stilbene, **3**, and (*E*,*E*,*E*,*E*)-1,4-bis(4-[4-{bis(4-methoxyphenyl)amino}styryl]styryl)benzene, **4**, have been oxidized to their mono- and dications using tris(4-bromophenyl)aminium hexachloroantimonate. The intervalence charge-transfer (IVCT) band of $\mathbf{1}^+$ is narrow and asymmetric and exhibits only weak solvatochromism. Analysis of this band indicates that $\mathbf{1}^+$ is a class-III or class-II/III borderline mixed-valence species. In contrast, a broad, strongly solvatochromic IVCT band is observed for $\mathbf{2}^+$, indicating that this species is a class-II mixed-valence species. The assignment of $\mathbf{1}^+$ and $\mathbf{2}^+$ as symmetric class-III and unsymmetric class-II species, respectively, is also supported by AM1 calculations. Hush analysis of the IVCT bands of both $\mathbf{1}^+$ and $\mathbf{2}^+$ gives larger electronic couplings, *V*, than for their analogues in which the double bonds are replaced with triple bonds. The diabatic electron-transfer distance, *R*, in $\mathbf{1}^+$ can be estimated by comparison of the *V* estimated by Hush analysis and from the IVCT maximum; it is considerably less than the geometric N−N separation, a result supported by quantum-chemical estimates of *R* for $\mathbf{1}^+$−$\mathbf{4}^+$. In $\mathbf{3}^+$ and $\mathbf{4}^+$, the IVCT is largely obscured by an intense absorption similar to a band seen in the corresponding dications and to that observed in the monocation of a model compound, (*E*,*E*,*E*)-1-{bis(4-methoxyphenyl)amino}-4-[4-{4-(4-*tert*-butylstyryl)styryl}styryl]benzene, **5**, containing only one nitrogen redox center; we attribute this band to a bridge-to-N^+ transition. The corresponding dications $\mathbf{1}^{2+}$−$\mathbf{4}^{2+}$ show a complementary trend in the coupling between redox centers: the shortest species is diamagnetic, while the dication with the longest bridge behaves as two essentially noninteracting radical centers.

Introduction

Mixed-valence (MV) compounds are comprised of two or more linked redox centers in different formal oxidation states.[1,2] Since Hush first developed the theory linking optical electron transfer with the Marcus theory of thermal electron transfer,[3] there has been considerable interest in transition-metal MV systems as model systems for understanding electron-transfer processes. More recently, organic MV systems have attracted increasing interest; these materials tend to exhibit stronger intersite coupling than their transition-metal-based analogues,[4] and, in some cases, they provide insight into the behavior of organic electronic and optical materials. Many different redox centers have been investigated, including quinones and imides,[5,6] dioxaborines,[7] nitro groups,[8,9] and perchlorotriphenylmethyl centers[10,11] in anionic organic MV systems, and hydrazines,[12,13] 1,4-dialkoxybenzenes,[14,15] and various alkylamines[16,17] in cationic systems. Triarylamine MV species have been the focus of a number of studies;[18−33] triarylamines may be readily

† Georgia Institute of Technology.
‡ University of Arizona.

(1) Robin, M. B.; Day, P. *Adv. Inorg. Chem. Radiochem.* **1967**, *10*, 247.
(2) Allen, G. C.; Hush, N. S. *Prog. Inorg. Chem.* **1967**, *8*, 357.
(3) Hush, N. S. *Prog. Inorg. Chem.* **1967**, *8*, 391.
(4) Nelsen, S. F.; Tran, H. Q.; Nagy, M. A. *J. Am. Chem. Soc.* **1998**, *120*, 298.
(5) Jozefiak, T. H.; Miller, L. L. *J. Am. Chem. Soc.* **1987**, *109*, 6560.
(6) Rak, S. F.; Miller, L. L. *J. Am. Chem. Soc.* **1992**, *114*, 1388.
(7) Risko, C.; Barlow, S.; Coropceanu, V.; Halik, M.; Brédas, J.-L.; Marder, S. R. *Chem. Commun.* **2003**, 194.
(8) Nelsen, S. F.; Konradsson, A. E.; Weaver, M. N.; Telo, J. P. *J. Am. Chem. Soc.* **2003**, *125*, 12493.
(9) Nelsen, S. F.; Weaver, M. N.; Zink, J. I. *J. Am. Chem. Soc.* **2005**, *127*, 10611.
(10) Bonvoisin, J.; Launay, J.-P.; Rovira, C.; Veciana, J. *Angew. Chem., Int. Ed. Engl.* **1994**, *33*, 2106.
(11) Sedó, J.; Ruiz, D.; Vidal-Gancedo, J.; Rovira, C.; Bonvoisin, J.; Launay, J.-P.; Veciana, J. *Synth. Met.* **1997**, *85*, 1651.
(12) Nelsen, S. F.; Chang, H.; Wolff, J. J.; Adamus, J. *J. Am. Chem. Soc.* **1993**, *115*, 12276.
(13) Nelsen, S. F.; Ismagilov, R. F.; Powell, D. R. *J. Am. Chem. Soc.* **1996**, *118*, 6313.
(14) Rosokha, S. V.; Sun, D.-L.; Kochi, J. K. *J. Phys. Chem. A* **2002**, *106*, 2283.
(15) Lindeman, S. V.; Rosokha, S. V.; Sun, D.; Kochi, J. K. *J. Am. Chem. Soc.* **2002**, *124*, 843.
(16) Nelsen, S. F.; Tran, H. Q. *J. Phys. Chem. A* **1999**, *103*, 8139.
(17) Bailey, S. E.; Zink, J. I.; Nelsen, S. F. *J. Am. Chem. Soc.* **2003**, *125*, 5939.
(18) Bonvoisin, J.; Launay, J.-P.; Van der Auweraer, M.; De Schryver, F. C. *J. Phys. Chem.* **1994**, *98*, 5052.

10.1021/ja054136e CCC: $30.25

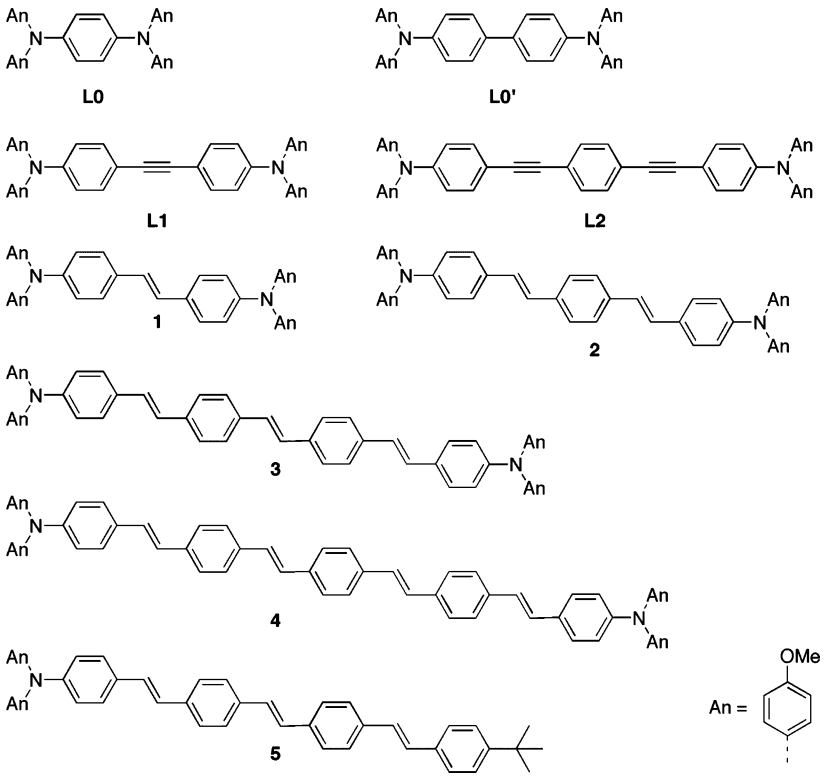

Figure 1. Structures of bis(triarylamines) considered in this work. The MV cations of **L0**, **L0′**, **L1**, and **L2** have previously been studied by Lambert and Nöll,[22] while those of **1**−**4** are the focus of the present work. The structure of the monoamine model compound, **5**, is also shown.

combined with a wide range of bridging groups and, with appropriate substitution patterns, can be converted to rather stable radical cations at only moderate oxidizing potentials.[34,35] Moreover, bis(triarylamine) derivatives are used as hole-transport agents in organic electronics applications,[36−39] the charge-transfer process involving electron hopping between neutral molecules and the corresponding MV radical cation.

Lambert and Nöll have studied the MV properties of a variety of bis(triarylamine) systems in which the terminal aryl groups have methoxy groups in the 4-position, including those with phenylene, biphenyl, and phenylene−ethynylene bridging groups;[22,25,32] additionally, several computational analyses have been published on these compounds.[24,27,29] The phenylene−ethynylene-bridged species $\mathbf{L1}^+$ and $\mathbf{L2}^+$ (Figure 1) appear to be Robin-Day[1] class-II (localized) MV compounds. The intervalence (ICVT) absorptions of shorter species with phenylene ($\mathbf{L0}^+$,[40] Figure 1) or biphenyl ($\mathbf{L0'}^+$) bridges show unusual markedly unsymmetrical profiles; it was originally suggested that these line shapes indicated localized species close to the class-II/III borderline,[22,41−43] but subsequent studies show these profiles are consistent with class-III systems exhibiting strong coupling of the electron transfer to symmetrical vibrations.[27] Comparison of UV-photoelectron and IVCT data allows one to estimate very small barriers for intramolecular electron transfer in these species, confirming them to be at least very close to the class II/III borderline, or possibly to belong to class III.[31] Recently, crystalline salts of two examples of these cations — 1,4-bis(diphenylamino)benzene[44] and 4,4′-bis[phenyl-(2,4-dimethylphenyl)amino]biphenyl[30] — have been isolated and shown using X-ray crystallography to have symmetrical structures consistent with assignment to class III. Vibrational studies confirm that these two species and the 4,4′-bis[phenyl-(2,4-dimethylphenyl)amino]biphenyl cation (TPD^+) belong to class III.[30,44,45] More recently still, we have reported the first example of a MV bis(triarylamine) with a vinylene bridge, $\mathbf{1}^+$, which

(19) Stickley, K. R.; Blackstock, S. C. *Tetrahedron Lett.* **1995**, *36*, 1585.
(20) Lambert, C.; Nöll, G.; Schmälzlin, E.; Meerholz, K.; Bräuchle, C. *Chem. Eur. J.* **1998**, *4*, 2129.
(21) Lambert, C.; Nöll, G. *Angew. Chem., Int. Ed.* **1998**, *37*, 2107.
(22) Lambert, C.; Nöll, G. *J. Am. Chem. Soc.* **1999**, *121*, 8434.
(23) Lambert, C.; Nöll, G.; Hampel, F. *J. Phys. Chem. A* **2001**, *105*, 7751.
(24) Coropceanu, V.; Malagoli, M.; André, J. M.; Brédas, J. L. *J. Chem. Phys.* **2001**, *115*, 10409.
(25) Lambert, C.; Nöll, G.; Schelter, J. *Nat. Mater.* **2002**, *1*, 69.
(26) Lambert, C.; Nöll, G. *Chem. Eur. J.* **2002**, *8*, 3467.
(27) Coropceanu, V.; Malagoli, M.; André, J. M.; Brédas, J. L. *J. Am. Chem. Soc.* **2002**, *124*, 10519.
(28) Yano, M.; Ishida, Y.; Aoyama, K.; Tatsumi, M.; Sato, K.; Shiomi, D.; Ichimura, A.; Takui, T. *Synth. Met.* **2003**, *137*, 1275.
(29) Coropceanu, V.; Lambert, C.; Nöll, G.; Brédas, J. L. *Chem. Phys. Lett.* **2003**, *373*, 153.
(30) Low, P. J.; Paterson, M. A. J.; Puschmann, H.; Goeta, A. E.; Howard, J. A. K.; Lambert, C.; Cherryman, J. C.; Tackley, D. R.; Leeming, S.; Brown, B. *Chem.—Eur. J.* **2004**, *10*, 83.
(31) Coropceanu, V.; Gruhn, N. E.; Barlow, S.; Lambert, C.; Durivage, J. C.; Bill, T. G.; Nöll, G.; Marder, S. R.; Brédas, J.-L. *J. Am. Chem. Soc.* **2004**, *126*, 2727.
(32) Lambert, C.; Amthor, S.; Schelter, J. *J. Phys. Chem. A* **2004**, *108*, 6474.
(33) Lambert, C.; Risko, C.; Coropceanu, V.; Schelter, J.; Amthor, S.; Gruhn, N. E.; Durivage, J. C.; Brédas, J. L. *J. Am. Chem. Soc.* **2005**, *127*, 8508.
(34) Seo, E. T.; Nelson, R. F.; Fritsch, J. M.; Marcoux, L. S.; Leedy, D. W.; Adams, R. N. *J. Am. Chem. Soc.* **1966**, *88*, 3498.
(35) Dapperheld, S.; Steckhan, E.; Grosse-Brinkhaus, K.-H.; Esch, T. *Chem. Ber.* **1991**, *124*, 2557.
(36) Tang, C. W.; Van Slyke, S. A. *Appl. Phys. Lett.* **1987**, *51*, 913.
(37) Kido, J.; Kimura, M.; Nagai, K. *Science* **1995**, *267*, 1332.
(38) Bulovic, V.; Gu, G.; Burrows, P. E.; Forrest, S. R.; Thompson, M. E. *Nature* **1996**, *380*, 29.
(39) Borsenberger, P. M.; Weiss, D. S. *Organic Photoreceptors for Xerography*; Marcel Dekker: New York, 1998.
(40) For the first synthesis of $\mathbf{L0}^+$ and its isolation as a hexafluorophosphate salt, see: Selby, T. D.; Blackstock, S. C. *J. Am. Chem. Soc.* **1998**, *120*, 12155.
(41) Nelsen, S. F. *Chem. Eur. J.* **2000**, *2000*, 581.
(42) Demadis, K. D.; Hartshorn, C. M.; Meyer, T. J. *Chem. Rev.* **2001**, *101*, 2655.
(43) Brunschwig, B. S.; Creutz, C.; Sutin, N. *Chem. Soc. Rev.* **2002**, *31*, 168−184.
(44) Szeghalmi, A. V. et al. *J. Am. Chem. Soc.* **2004**, *126*, 7834.

Scheme 1. Synthesis of Compounds **1**−**4**

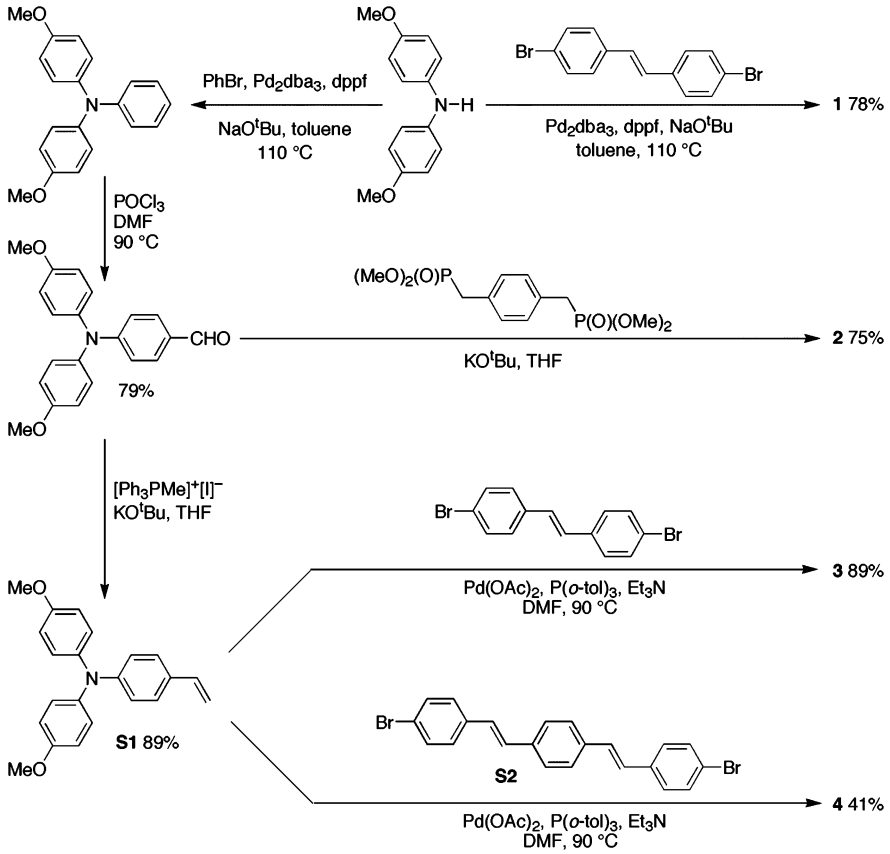

also has a markedly unsymmetrical IVCT band, and shown, using X-ray crystallography and vibrational spectroscopy, that it also belongs to class III, in contrast to its alkyne analogue, $\mathbf{L1}^+$.[46] Thus, it appears that bis(triarylamine)s with strongly asymmetric IVCT bands generally belong to class III.

Here we compare the spectroscopic and computational results for $\mathbf{1}^+$ with those for three additional longer phenylene−vinylene-bridged MV species ($\mathbf{2}^+$−$\mathbf{4}^+$) (Figure 1). We show that $\mathbf{2}^+$ is a class-II MV compound with stronger electronic coupling between the two redox centers, *V*, than in its alkyne analogue, $\mathbf{L2}^+$. In the case of $\mathbf{3}^+$ and $\mathbf{4}^+$, strong NIR bands are observed. At first sight, one might attribute these absorptions to IVCT bands and deduce rather large *V* in these species; however, we show, by comparison with similar features found in the spectra of the corresponding dications and of the monocation of a model compound containing a single amine redox center, $\mathbf{5}^+$ (Figure 1), that these features have a different origin.

Results and Discussion

Synthesis and Characterization of 1−5. Compounds **1**−**4** were synthesized using a combination of palladium-catalyzed C−N coupling,[47,48] Horner-Emmons,[49,50] and Heck[51,52] reactions, as shown in Scheme 1. (The synthesis of **1** is described elsewhere;[46] a very similar synthesis of **2** has recently been published,[53] and independent syntheses of several close analogues of **3**[54] and **4**[55] have recently appeared.) UV−vis data for the neutral compounds are tabulated in Table 1, along with electrochemical data and with spectroscopic data for the corresponding monocations and dications (vide infra). UV−vis spectra for the neutral species are very similar to those reported for other triarylamine-terminated phenylene−vinylene oligomers with the same chain lengths: for example, **4** shows $\lambda_{max} = 435$ nm ($\epsilon_{max} = 113\,000$ M^{-1} cm^{-1}); similar values of $\lambda_{max} = 437$ nm ($\epsilon_{max} = 99\,000$ M^{-1} cm^{-1}) have been reported for an analogue with unsubstituted phenyl end groups and with *n*-octyloxy groups on the central phenylene ring of the bridge. To better understand the spectra of $\mathbf{3}^+$ and $\mathbf{4}^+$ (vide infra), we were interested in a model compound in which only one triarylamine group was attached to a phenylene−vinylene chain. Hence, we also synthesized compound **5**, using the synthetic route shown in Scheme 2; data for **5** and $\mathbf{5}^+$ are also included in Table 1.

Electrochemistry. Cyclic voltammetry (CV; Table 1) shows that two electrons can be removed readily and reversibly from each of the compounds **1**−**4**. In the case of the stilbene species, **1**, two distinct potentials are resolvable corresponding to oxidation to monocation ($E_{1/2}{}^{+/0}$) and dication ($E_{1/2}{}^{2+/+}$); the separation between these potentials, $\Delta E_{1/2} = E_{1/2}{}^{2+/+} - E_{1/2}{}^{+/0}$, was more accurately determined using differential pulse voltammetry (DPV) to be 134 mV. The more facile first oxidation

(45) Littleford, R. E.; Paterson, M. A. J.; Low, P. J.; Tackley, D. R.; Jayes, L.; Dent, G.; Cherryman, J. C.; Brown, B.; Smith, W. E. *Phys. Chem. Chem. Phys.* **2004**, *6*, 3257.
(46) Barlow, S. et al. *Chem. Commun.* **2005**, 764.
(47) Driver, M. S.; Hartwig, J. F. *J. Am. Chem. Soc.* **1996**, *118*, 7217.
(48) Wolfe, J. P.; Wagaw, S.; Buchwald, S. L. *J. Am. Chem. Soc.* **1996**, *118*, 7215.
(49) Horner, L. *Chem. Ber.* **1958**, *83*, 733.
(50) Wadsworth, W. S.; Emmons, W. D. *J. Am. Chem. Soc.* **1961**, *83*, 1733.
(51) Heck, R. F. *J. Am. Chem. Soc.* **1968**, *90*, 5518.
(52) de Meijere, A.; Meyer, F. E. *Angew. Chem., Int. Ed. Engl.* **1994**, *33*, 2379.
(53) Kauffman, J. M.; Moyna, G. *J. Org. Chem.* **2003**, *68*, 839.
(54) Li, C.-L.; Shieh, S.-J.; Lin, S.-C.; Liu, R.-S. *Org. Lett.* **2003**, *5*, 1131.
(55) Detert, H.; Sadovski, O. *Synth. Met.* **2003**, *138*, 185.

Table 1. Electrochemical (0.1 M $[^nBu_4N]^+[PF_6]^-/CH_2Cl_2$) and UV−vis−NIR Spectroscopic (CH_2Cl_2) Data for **1**−**5** and Their Cations and Dications

	$E_{1/2}/V$[a]				$\bar{\nu}_{max}$ (ϵ_{max})/10^3 cm^{-1} (10^3 M^{-1} cm^{-1})		
	+/0	2+/+	3+/2+	4+/3+	neutral	monocation[b]	dication[b]
1	+0.08	+0.22	−	−	25.1 (54), 32.7 (27)	6.1 (39), 16.2 (34)	11.1 (129), 15.9 (13), 20.0 (10)
2	+0.20[c]		+0.81	−	23.8 (76), 33.3 (36)	6.1 (16), 10.2 (6), 14.6 (23)	9.3 (63), 14.3 (28)
3	+0.20[c]		+0.69	−	23.3 (100), 32.7 (37)	8.7 (11), 14.2 (14), 16.0 (13)	8.6 (30), 14.2 (29), 16.3 (25)
4	+0.18[c]		+0.65	+0.77	23.0 (113), 32.8 (31)	8.5 (15), 14.3 (14), 17.9 (12)	8.5 (34), 14.2 (29)
5	+0.21	+0.66	−	−	24.0 (88), 33.0 (26)	8.5 (17), 14.3 (14), 15.7 (14)	−

[a] Electrochemical half-wave potentials corresponding to successive oxidations of the molecule, referenced to $FeCp_2^{+/0}$. [b] The high-energy (>24 000 cm^{-1}) parts of the spectra of the cationic species are not reported due to overlap with the absorptions of excess neutral species (in the case of monocations) and with the tris(4-bromophenyl)amine side product. [c] No separation resolved between first and second oxidations.

Scheme 2. Synthesis of Compound **5**

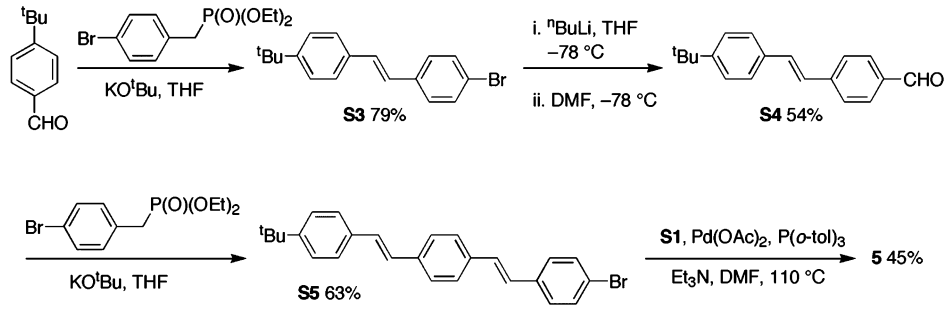

observed in **1** versus its longer homologues presumably reflects greater stabilization of this cation through delocalization. For **2**−**4**, $\Delta E_{1/2}$ is too small to be evident in the CV and was also undetectable by DPV; the CVs are characteristic of species undergoing two independent one-electron redox processes at very similar potentials. Lambert and Nöll obtained redox splittings of 150 and 60 mV through digital simulations of the CVs for **L1** and **L2**, respectively, in the same electrolyte medium.[22] In addition, they reported a linear correlation between $\Delta E_{1/2}$ for their compounds and the electronic coupling, V, in the corresponding MV monocations, as determined by Hush analysis of their IVCT absorptions.[22] However, it should be noted that $\Delta E_{1/2}$ is affected by many factors besides electronic coupling, and such a correlation is not necessarily expected.[56] In the species with longer phenylene−vinylene bridges, **2**−**4**, and in the monoamine model compound, **5**, additional less reversible (reduced I_{red}/I_{ox}, increased $E_{ox} - E_{red}$) redox features are observable at more strongly oxidizing potentials. These additional features presumably correspond to bridge-based oxidations and, accordingly, become increasingly facile with increased length of the bridging group; this behavior of increased ease of oxidation with increased chain length is seen in other oligo(phenylenevinylene) derivatives (for example, see ref 57).

Electronic Spectra of the Monocations and Dications of 1−**5.** Tris(4-bromophenyl)aminium hexachloroantimonate was chosen as an oxidizing agent for the generation of the monocations and dications of the bis(triarylamine) species; the salt is easily weighed out stoichiometrically and readily able to effect oxidation of all of our bis(triarylamine)s to both mono- and dications ($E_{1/2} = +0.70$ V vs ferrocenium/ferrocene in dichloromethane[58]), and the side product of oxidation, tris(4-bromophenyl)amine, shows neither a vis−NIR absorption[59] nor any electron spin resonance (ESR) signal. Solutions containing the monocations were obtained by the addition of tris(4-bromophenyl)aminium hexachloroantimonate solution to large excesses (>10 equiv) of the neutral bis(triarylamine) solutions, while the dications were generated by the addition of 2 equiv of oxidizing agent to the amines. Similar spectra were obtained using solutions of isolated crystalline salts of the mono-[46] and dications[60] for **1**. These solutions were then investigated using vis−NIR (Figure 2) and ESR spectroscopy.

The MV monocations of the bis(triarylamines) all show intense absorptions in the NIR. In the cases of $\mathbf{1}^+$ and $\mathbf{2}^+$, these features are observed at considerably lower energy than the lowest energy absorption of the corresponding dications and can be attributed to the IVCT bands.[61] Some parameters characterizing these bands are collected in Table 2 along with those for their alkyne analogues, $\mathbf{L1}^+$ and $\mathbf{L2}^+$. Lambert and Nöll previously reported the corresponding parameters for $\mathbf{L1}^+$ and $\mathbf{L2}^+$ electrochemically generated in 0.1 M $[^nBu_4N]^+[PF_6]^-/CH_2Cl_2$,[22] and we have reported line-shape data for $\mathbf{1}^+$ chemically generated in 0.1 M $[^nBu_4N]^+[PF_6]^-/CH_2Cl_2$;[46] the line-shape parameters depend only slightly on the presence or absence of electrolyte, although the absorption maxima are red-

(56) For examples of strong solvent and counterion dependence of $\Delta E_{1/2}$, see: (a) Barriere, F.; Camire, N.; Geiger, W. E.; Mueller-Westerhoff, U. T.; Sanders, R. *J. Am. Chem. Soc.* **2002**, *124*, 7262. For an example of a pair of isoelectronic mixed-valence species where estimating the electronic coupling from $\Delta E_{1/2}$ would lead to the opposite conclusion to that indicated by UV−vis−NIR spectroscopy, compare the dicobalt and dimanganese species of: (b) Manriquez, J. M.; Ward, M. D.; Reiff, W. M.; Calabrese, J. C.; Jones, N. L.; Carroll, P. J.; Bunel, E. E.; Miller, J. S. *J. Am. Chem. Soc.* **1995**, *117*, 6182. (c) Jones, S. C.; Hascall, T.; Barlow, S.; O'Hare, D. *J. Am. Chem. Soc.* **2002**, *124*, 11610, respectively.

(57) Peeters, E.; van Hal, P. A.; Knol, J.; Brabec, C. J.; Sariciftci, N. S.; Hummelen, J. C.; Janssen, R. A. J. *J. Phys. Chem. B* **2000**, *104*, 10174.

(58) Connelly, N. G.; Geiger, W. E. *Chem. Rev.* **1996**, *96*, 877.

(59) The absorption maximum for the neutral tris(4-bromophenyl)amine molecule is at 312 nm (Schmidt, W.; Steckhan, E. *Chem. Ber.* **1980**, *113*, 577).

(60) Zheng, S. et al. Submitted.

(61) The spectra for $\mathbf{1}^{2+}$ and $\mathbf{2}^{2+}$ can also be compared to those of the dications of stilbene and 1,4-bis(styryl)benzene which have low-energy maxima at 8850 and 8720 cm^{-1}, respectively (Spangler, C. W.; Hall, T. J. *Synth. Met.* **1991**, *44*, 85. Spangler, C. W.; Liu, P.-K.; Nickel, E. G. *AIP Conference Proceedings* **1992**, *262*, 28). The maximum for the 1,4-bis(4-methylstyryl)-benzene monocation is at 8330 cm^{-1} (Sakamoto, A.; Furukawa, Y.; Tasumi, M. *J. Phys. Chem. B* **1997**, *101*, 1726).

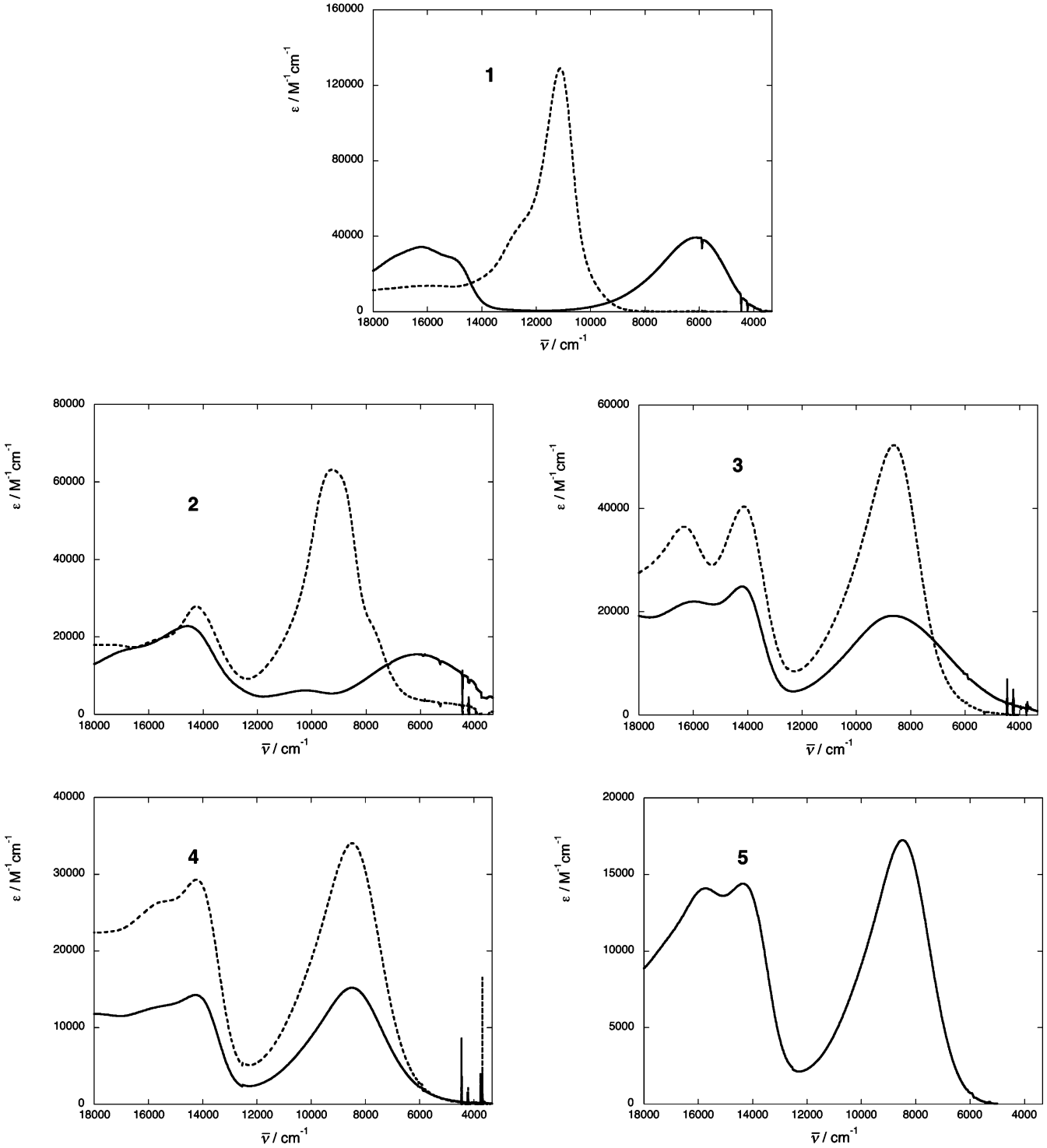

Figure 2. Spectra in dichloromethane of the mono- (solid lines) and dications (broken lines) of **1**−**4**, along with the spectrum of the monocation of **5** (see Experimental Section for details). Note each graph has a different vertical scale.

shifted somewhat in the presence of electrolyte (least so in the case of $\mathbf{1}^+$, consistent with its weaker solvatochromism; vide infra).

The asymmetry of the IVCT bands is characterized in Table 2 by $\bar{\nu}_{1/2}$[high]/$\bar{\nu}_{1/2}$[low], where $\bar{\nu}_{1/2}$[high] and $\bar{\nu}_{1/2}$[low] are twice the half-widths on the high- and low-energy side of the band, respectively;[22] for $\mathbf{1}^+$, the asymmetry is stronger than that for its alkyne analogue, $\mathbf{L1}^+$. The width of the bands can be compared directly through the values of $\bar{\nu}_{1/2}$[obs], or through comparison of the observed widths (or widths on the high-energy side) with the width expected from Hush theory for class-II compounds, $\bar{\nu}_{1/2}$[Hush], given in cm^{-1} by eq 1:

$$\bar{\nu}_{1/2}[\text{Hush}] = \sqrt{2310 \times \bar{\nu}_{\max}} \qquad (1)$$

where $\bar{\nu}_{\max}$ is also in cm^{-1}. In the case of $\mathbf{L1}^+$ in CH_2Cl_2, our data show that twice the width on the high-energy side, $\bar{\nu}_{1/2}$[high], somewhat exceeds the Hush limit, while $\bar{\nu}_{1/2}$[obs] is

Table 2. Parameters Relating to the IVCT Absorptions of $\mathbf{1}^+$, $\mathbf{2}^+$, $\mathbf{L1}^+$, and $\mathbf{L2}^+$ Acquired Using Chemical Oxidation with $[(4\text{-}BrC_6H_4)_3N]^+[SbCl_6]^-$

	CH_2Cl_2							MeCN
	$\bar{\nu}_{max}$/cm^{-1}	ϵ_{max}/M^{-1} cm^{-1}	$\bar{\nu}_{1/2}$[obs]/cm^{-1}	$\bar{\nu}_{1/2}$[Hush][a]/cm^{-1}	$\bar{\nu}_{1/2}$[high]/$\bar{\nu}_{1/2}$[low][b]	$\bar{\nu}_{1/2}$[high]/$\bar{\nu}_{1/2}$[Hush][c]	μ_{ge}[d]/D	$\bar{\nu}_{max}$/cm^{-1}
$\mathbf{1}^+$[e]	6080[e]	39 300	2760	3750	1.40	0.86	13.5	7010
$\mathbf{2}^+$	6130	15 510	4310[f]	3760	1[f]	1.15[f]	10.3	8200
$\mathbf{L1}^+$	5760	21 800	3460	3650	1.23	1.04	11.3	7930
$\mathbf{L2}^+$[g]	7780	5260	5180[f]	4240	1[f]	1.22[f]	5.85	9910

[a] Calculated according to eq 1. [b] Ratio of bandwidth on high-energy side to bandwidth on low-energy side. [c] Ratio of twice the bandwidth on the high-energy side to the bandwidth predicted by eq 1. [d] Transition dipole moment calculated from the IVCT band using eq 3 (vide infra). [e] Similar values ($\bar{\nu}_{max}$ = 6150 cm^{-1} and μ_{ge} = 13.0 D) were given for $\mathbf{1}^+$ in CH_2Cl_2 in a footnote to ref 66. [f] Some overlap with another transition on high-energy side; band was fitted acceptably to a symmetrical Gaussian, and so $\bar{\nu}_{1/2}$[high] was assumed to be equal to $\bar{\nu}_{1/2}$. [g] Reference 25 gives similar values ($\bar{\nu}_{max}$ = 8060 cm^{-1} and μ_{ge} = 6.2 D) for $\mathbf{L2}^+$ generated in CH_2Cl_2 by oxidation with $SbCl_5$.

marginally less than the Hush limit; Lambert and Nöll showed that, in 0.1 M $[^nBu_4N]^+[PF_6]^-/CH_2Cl_2$, both $\bar{\nu}_{1/2}$[high] and $\bar{\nu}_{1/2}$[obs] exceed the Hush limit.[22] However, for $\mathbf{1}^+$, both $\bar{\nu}_{1/2}$[obs] and $\bar{\nu}_{1/2}$[high] are considerably less than $\bar{\nu}_{1/2}$[Hush] with or without electrolyte present; indeed, the $\bar{\nu}_{1/2}$[obs] values and the ratios of $\bar{\nu}_{1/2}$[high]/$\bar{\nu}_{1/2}$[Hush] are less than that for any of the species reported by Lambert and Nöll in ref 22 (line-shape data for $\mathbf{1}^+$ in electrolyte solution are given in ref 46). Moreover, the IVCT band of $\mathbf{1}^+$ is considerably less solvatochromic than that of $\mathbf{L1}^+$; that of $\mathbf{1}^+$ is blue-shifted by some 930 cm^{-1} between dichloromethane and acetonitrile, whereas the corresponding blue-shift seen for $\mathbf{L1}^+$ is ca. 2170 cm^{-1} (more extensive solvatochromic data for $\mathbf{1}^+$ and $\mathbf{L1}^+$ are given in the Supporting Information of ref 46). The solvatochromism of $\mathbf{1}^+$ is similar in magnitude to that seen for the bis(diphenylamino)-benzene cation (860 cm^{-1} shift from dichloromethane to acetonitrile), which has been shown to belong to class III using crystallographic and vibrational data.[44] The differences in the asymmetry, width, and solvatochromism of the IVCT bands of $\mathbf{1}^+$ and $\mathbf{L1}^+$ are consistent with their assignment to classes III and II, respectively, an assignment also supported by vibrational data (the IR spectrum of a solution of $\mathbf{L1}^+$ in dichloromethane, generated in the same way as the samples for electronic spectroscopy, shows an alkyne stretch, clearly indicating a broken symmetry structure).[46]

The IVCT band of $\mathbf{2}^+$ is qualitatively similar to that of $\mathbf{L2}^+$ in terms of symmetry (both bands were fitted with symmetrical Gaussians to deconvolute them from other overlapping bands, but the IVCT band shown for $\mathbf{2}^+$ in Figure 2 is clearly at least approximately symmetrical), width versus the Hush limit, and solvatochromism, all of which are consistent with assignment of both species to class II. The main differences are that the transition for $\mathbf{2}^+$ is at lower energy, indicating a smaller reorganization energy, and has a much higher transition dipole moment than that for $\mathbf{L2}^+$.

In the cases of $\mathbf{3}^+$ and $\mathbf{4}^+$, rather intense (ϵ_{max} = ca. 10^4 M^{-1} cm^{-1}) bands are observed in the NIR (ca. 9000 cm^{-1}). The unwary might assign these near-IR bands to IVCT and deduce rather strong electronic coupling between the two redox centers using Hush analysis. However, absorptions at similar energy, with approximately twice the absorptivity, are seen in $\mathbf{3}^{2+}$ and $\mathbf{4}^{2+}$, and a band with similar energy and absorptivity is also seen in $\mathbf{5}^+$, a compound in which there is only one triarylamine center and where, therefore, a triarylamine-to-triarylaminium IVCT transition is not possible. We, therefore, assign these transitions to charge transfer from the highest bridge-based orbital to the terminal donor radical cation (B → D$^+$). The NIR band of $\mathbf{3}^+$ is, however, considerably broader on the low-energy side than those of $\mathbf{3}^{2+}$ or $\mathbf{5}^+$; presumably, this is due to overlap between the B → D$^+$ transition and a weaker lower-energy IVCT band. In contrast, the line shapes of the low-energy band of $\mathbf{4}^+$ are very similar to those of $\mathbf{4}^{2+}$, suggesting the IVCT in this species is much weaker than in $\mathbf{3}^+$. The situation of $\mathbf{3}^+$ and $\mathbf{4}^+$ strongly resembles that of $[Ar(p\text{-}C_6H_4)_4Ar]^+$ {Ar = 2,5-dimethoxy-4-methylphen-1-yl}, which has its lowest energy electronic absorption at 7810 cm^{-1}, while the corresponding dication absorbs at 7750 cm^{-1} with ca. 1.5 times the absorptivity, both bands being assigned to B → D$^+$ transitions.[14] Moreover, a transition in $\mathbf{L2}^+$ seen at ca. 12 000 cm^{-1} has also been attributed to a B → D$^+$ transition; the transition becomes red-shifted when the central benzene ring is replaced by anthracene or dimethoxybenzene,[25,32,62] or by *trans*-$Pt(PEt_3)_2$.[63] A transition at 10 200 cm^{-1} in the spectrum of $\mathbf{2}^+$ (in dichloromethane; the band is not seen in acetonitrile, presumably due to overlap with the blue-shifted IVCT) is possibly due to a similar B → D$^+$ transition; the band energy (i.e., higher than that for $\mathbf{3}^+$ and $\mathbf{4}^+$ and lower than that for $\mathbf{L2}^+$) is certainly broadly consistent.

Higher energy transitions are seen at ca. 14 000−16 500 cm^{-1} for all compounds. Similar bands are seen for Lambert and Nöll's compounds and were assigned to localized transitions within the Ar_2N^+ units;[22] the mononuclear triarylaminium species $[(4\text{-}MeOC_6H_4)_3N]^+$ and $[(4\text{-}MeC_6H_4)_3N]^+$ absorb at ca. 14 000 and 15 000 cm^{-1}, respectively, in acetonitrile.[64] Significantly, for $\mathbf{1}^+$, this band is considerably blue-shifted from those of simple triarylamine radical cations; this has also seen in the case of other class-III bis(triarylamine) derivatives, such as $\mathbf{L0'}^+$ and other bis(diarylamino)biphenyl cations;[22,30] TD-DFT calculations suggest that in these systems the transitions can be regarded as transitions from the HOMO (using the orbital label from the neutral molecule) to a bridge-based LUMO.[30] In the species with longer π-bridges, and in $\mathbf{L1}^+$ and $\mathbf{L2}^+$, the energies of these bands more closely approach those of the parent triarylaminium species; moreover, the band is seen at similar energies in mono- and dications, and in $\mathbf{3}^+$ and $\mathbf{4}^+$, the intensity in the dication is approximately twice that in the monocation. These observations are entirely consistent with $\mathbf{1}^+$ having more delocalized structures than $\mathbf{L1}^+$ and than the species with longer bridges.[65]

(62) A similar assignment has been made for the low-energy band of a bis(hydrazine) MV species with an anthracene bridge (Nelsen, S. F.; Ismagilov, R. F.; Powell, D. R. *J. Am. Chem. Soc.* **1998**, *120*, 1924).
(63) Jones, S. C.; Coropceanu, V.; Barlow, S.; Kinnibrugh, T.; Timofeeva, T.; Brédas, J.-L.; Marder, S. R. *J. Am. Chem. Soc.* **2004**, *126*, 11782.
(64) Walter, R. I. *J. Am. Chem. Soc.* **1966**, *88*, 1923.
(65) The differences in profile and similarity in intensity for the band at ca. 14 000 cm^{-1} in $\mathbf{2}^+$ and $\mathbf{2}^{2+}$ suggest $\mathbf{2}^+$, although still belonging to class II, is more delocalized than $\mathbf{L2}^+$, $\mathbf{3}^+$, and $\mathbf{4}^+$.

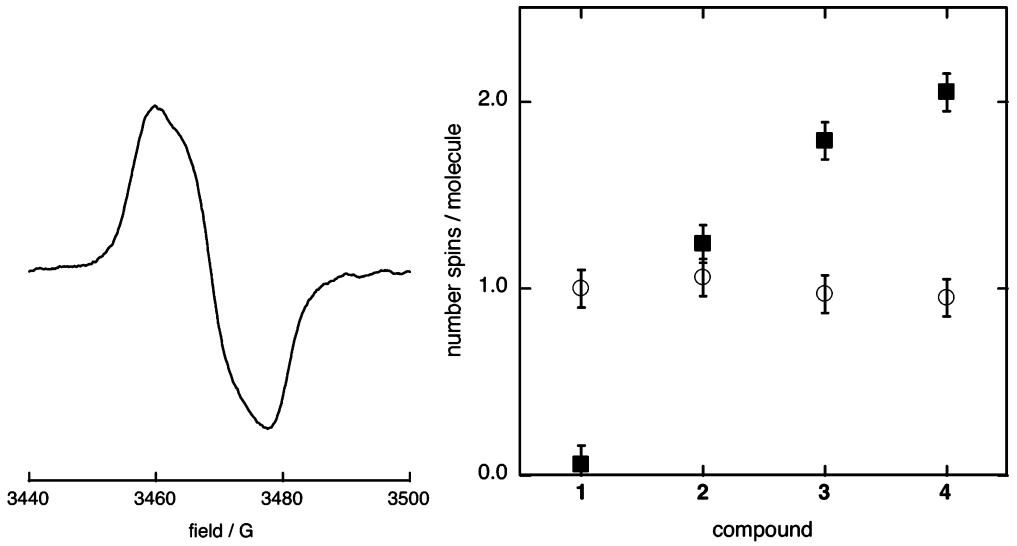

Figure 3. Left: First derivative ESR spectrum of $\mathbf{4}^{2+}$ generated in situ in CH_2Cl_2. Right: Plot showing numbers of spin-$^1/_2$ centers per molecule determined by integration of the ESR signals for mono- (open circles) and dications (solid squares) of **1**−**4**, normalized to unity for $\mathbf{1}^+$.

Electron-Spin Resonance Spectra of Mono- and Dications. Room-temperature ESR spectra were acquired for the in situ generated dichloromethane solutions of $\mathbf{2}^+$−$\mathbf{5}^+$ and $\mathbf{2}^{2+}$−$\mathbf{4}^{2+}$. We have previously reported the spectrum of a solution of $\mathbf{1}^+[SbF_6]^-$ and of in situ generated $\mathbf{L1}^+$.[46] All the monocations show spectra centered at $g = 2.004$ (Ph_3N^+ is reported at $g = 2.003$[67]). The monocation spectra are poorly resolved and, hence, not particularly useful in giving insight into the delocalization in the monocations. While the ESR spectra of several tris(aryl)-aminium radical cations, such as $[(4\text{-}MeOC_6H_4)_3N]^+$, show very well-resolved ^1H coupling, the lack of resolution in the present cases is not particularly surprising given the number of inequivalent protons; for example, the poor resolution of the spectrum of the tris(biphenyl-4-yl)aminium cation has been attributed to the large number of inequivalent protons.[68] In the case of $\mathbf{1}^+$ and $\mathbf{L1}^+$, we were able to resolve coupling; we interpret this as arising from two equivalent $I = 1$ centers with a coupling constant, A_N, of ca. 4.3 G, indicating these cations are either class-III or class-II with a room-temperature intermolecular exchange rate in excess of 10^7 s^{-1}. The coupling constant is consistent with these radicals being triarylaminium-centered; $A_N = 8.97$ G for $[(4\text{-}MeOC_6H_4)_3N]^+$ in MeCN.[34] Our model mononuclear triarylaminium species, $\mathbf{5}^+$, shows a poorly resolved triplet characterized by $A_N = 8.6$ G, indicating the oxidation in this species is also triarylamine-centered.

The ESR spectra of the dications afford more interesting information; $\mathbf{2}^{2+}$−$\mathbf{4}^{2+}$ all show structureless features at $g = 2.004$ (as an example, the ESR spectrum of $\mathbf{4}^{2+}$ is shown in Figure 3), while $\mathbf{1}^{2+}$ shows only a very weak signal that we attribute to an impurity. Spin concentrations for solutions of these dications were estimated by double integration of the first-derivative spectra of solutions of known concentration and comparison with those from monocation solutions at comparable known concentrations. These integrals correspond to values equivalent to 1.2, 1.8, and 2.1 (±0.1) $S = {}^1/_2$ centers for $\mathbf{2}^{2+}$, $\mathbf{3}^{2+}$, and $\mathbf{4}^{2+}$, respectively. In combination with the diamagnetic behavior of $\mathbf{1}^{2+}$, these data indicate a gradual transition from strongly coupled redox centers to essentially noninteracting radical centers in the longest species (Figure 3), thus presenting a similar trend to that seen in the monocation NIR spectra.

Optimized Geometry of Neutral and Cationic Species. The AM1-optimized geometries for neutral **1** and **2** are shown in Figure 4. The phenylene−vinylene bridges of neutral **1**−**4** are somewhat twisted in a helical fashion, with dihedral angles of ca. 20° between the phenyl rings and the vinylene units; however, planarization of the bridges only costs energy of the order of *kT*. The amines are slightly pyramidal; the angle sum around the nitrogen atoms is ca. 357°. DFT calculations produce very similar results for the neutral species with the main difference being a less pronounced twist in the phenylene−vinylene bridges and nonpyramidal amines.

Figure 4 also shows the AM1/CI structures for $\mathbf{1}^+$ and $\mathbf{2}^+$; in the cases of all four species studied, there are significant geometric changes relative to the neutral species (details of the bond length changes are tabulated in the Supporting Information). $\mathbf{1}^+$ maintains a symmetric structure and is planarized both at nitrogen and in the bridge. The $N-C_{stilbene}$ bonds decrease by 0.046 Å on oxidation, and the C−C bonds in the stilbene bridge change toward a quinoid-like arrangement. The net charge is symmetrically distributed over the whole structure. In contrast, the AM1/CI structures of $\mathbf{2}^+$−$\mathbf{4}^+$ show definitively broken symmetry; in each case, one of the nitrogen centers and a stilbene unit become planarized with a similar bond length pattern to $\mathbf{1}^+$, while the remainder of the system maintains a twisted neutral-like structure. The excess charge is localized solely within the planarized section of the structure.

Electron Transfer Distance and Electronic Coupling. Hush showed that the electronic coupling, *V*, between redox centers in a MV species can be derived from the IVCT band according to

$$V = \frac{\mu_{ge}\bar{\nu}_{max}}{eR} \qquad (2)$$

where *R* is the effective separation between donor and acceptor

(66) Heckmann, A.; Lambert, C.; Goebel, M.; Wortmann, R. *Angew. Chem., Int. Ed.* **2004**, *43*, 5851.
(67) Bamberger, S.; Hellwinkel, D.; Neugebauer, F. A. *Chem. Ber.* **1975**, *108*, 2416.
(68) Pearson, G. A.; Rocek, M.; Walter, R. I. *J. Phys. Chem.* **1978**, *82*, 1185.

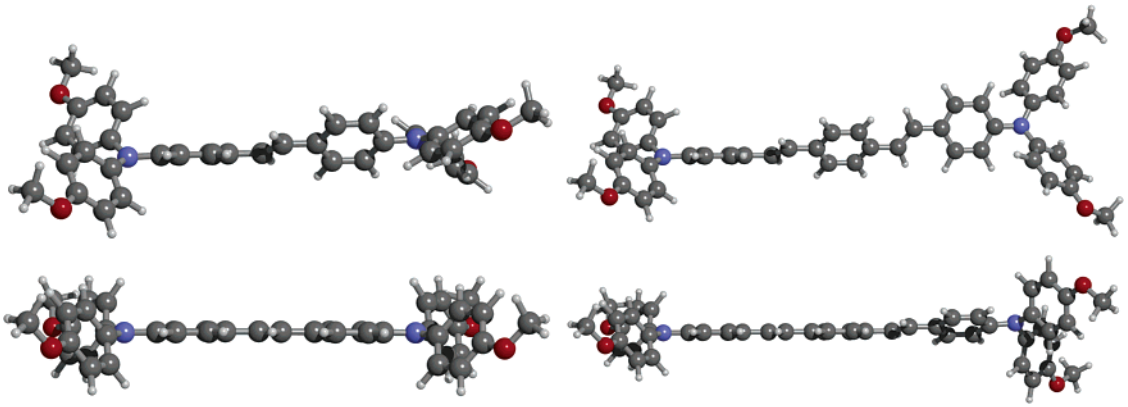

Figure 4. Ball-and-stick model of geometries of **1** (top left), **2** (top right), $\mathbf{1}^+$ (lower left), and $\mathbf{2}^+$ (lower right) according to AM1 (neutral) and AM1/CI (radical cation) levels of theory.

(diabatic states), and μ_{ge} is the transition dipole moment associated with the transition and given, in Debye, by

$$\mu_{ge} = 0.09584\sqrt{\frac{\int \epsilon(\bar{\nu})\mathrm{d}\bar{\nu}}{\bar{\nu}_{max}}} \quad (3)$$

where $\bar{\nu}_{max}$ and $\epsilon(\bar{\nu})$ are in cm^{-1} and $M^{-1}\ cm^{-1}$, respectively. In the case of symmetric Gaussian IVCT bands, eqs 2 and 3 are often combined to give eq 4:

$$V = 0.0206\frac{\sqrt{\epsilon_{max}\bar{\nu}_{max}\bar{\nu}_{1/2}}}{R} \quad (4)$$

where R is in Å.[3,69] A problem in applying Hush's equation is in determining the appropriate value of the diabatic electron-transfer distance, R. In traditional inorganic MV systems, the metal−metal geometric separation is often used as an approximation, but in organic systems, there is more difficulty in defining the appropriate center of the charge-bearing unit. Moreover, in both organic and inorganic cases, any delocalization of the charge away from the formal charge-bearing center toward the bridging group (for the diabatic states) will lead to reduced R. For a class-III system, the coupling can also be obtained directly from the absorption maximum:

$$2V = \bar{\nu}_{max} \quad (5)$$

Thus, for a class-III system, one can input a value of V from eq 5 into eq 2 and solve for R (rather than estimating V from an assumed value of R); for $\mathbf{1}^+$, we obtain a value of $R = 5.67$ Å, considerably less than the geometric N−N distance of 12.23 Å, suggesting that the diabatic states cannot be regarded as centered on the nitrogen atoms, but are centered somewhat into the bridge. Unfortunately, analogous estimates of the appropriate value of R cannot be made for the class-II species $\mathbf{2}^+$−$\mathbf{4}^+$. However, R can be estimated in several other ways from computational and/or spectroscopic data. One possible method is to use eq 6:[27]

$$|\mu_{\pm}| = |eR/2| \quad (6)$$

where $\mu_{\pm}$ is the calculated transition dipole between adiabatic surfaces at the transition (crossing point of diabatic surfaces) geometry. An alternative estimate is given by eq 7:

$$R = \frac{\sqrt{\Delta\mu_{12}^2 + 4\mu_{ge}^2}}{e} \quad (7)$$

where μ_{ge} is the (experimental or calculated) transition dipole moment between the two adiabatic surfaces at the minimum-energy geometry, and $\Delta\mu_{12}$ is the difference in the static dipole moments of the two adiabatic states.[70,71]

To estimate R according to eq 6, ZINDO/CIS calculations were performed for $\mathbf{1}^+$−$\mathbf{4}^+$ using the neutral DFT geometry (chosen since it is symmetrical in each case); values of $\mu_{\pm}$ are given in Table 3, along with the derived values of R, the calculated transition energies, and configuration descriptions of the transitions. In each case, the transition between ground and first excited states can be well-described as a HOMO-1 → HOMO one-electron transition (using the molecular orbital labels from the neutral electronic configuration). The HOMO and HOMO-1 of **1** and **2** are shown in Figure 5 and consist of different symmetry combinations of nitrogen p orbitals, with some contribution from other atoms, particularly from the π-bridging unit in the HOMO.

We also estimated R according to eq 7 using experimental values of μ_{ge} (see Table 2) and values of $\Delta\mu_{12}$ obtained from

Table 3. Excitation Energies, E, and Transition Dipole Moments, for Compounds $\mathbf{1}^+$−$\mathbf{4}^+$ According to ZINDO/CIS Calculations at the Neutral AM1 Geometries, along with the Geometric N−N Distance (AM1, neutral), Diabatic Electron-Transfer Distances, R, and Estimated Adiabatic Electron-Transfer Distance, R_{12}

	E/eV	$\mu_{\pm}$/D	R_{NN}[a]/Å	$R_{[eq6]}$/Å	$R_{[eq7]}$/Å	R_{12}/Å
$\mathbf{1}^+$	0.389	21.0	12.23	8.78	5.92	1.88
$\mathbf{2}^+$	0.287	27.6	18.78	11.53	8.72	7.58
$\mathbf{3}^+$	0.249	32.5	25.32	13.58	–	10.68
$\mathbf{4}^+$	0.043	52.4	31.79	21.98	–	22.22
$\mathbf{L1}^+$	0.436	21.5	12.48[b]	8.98	–	–

[a] For $\mathbf{1}^+$−$\mathbf{4}^+$, we have used the AM1 neutral geometries since the parameter $R_{[eq6]}$ is also derived from a calculation at neutral geometry; the value taken for **1** is very close to that found in the crystal structure (12.24 Å).[46] However, AM1/CI optimization of the cation geometries gives extremely similar values (12.16, 18.77, 25.31, and 31.77 Å for $\mathbf{1}^+$, $\mathbf{2}^+$, $\mathbf{3}^+$, and $\mathbf{4}^+$, respectively), and so the couplings obtained from eq 2 (Table 4) are rather insensitive to whether neutral or cation values are used. [b] From ref 22; calculated using AM1/UHF for the cation.

(69) Creutz, C.; Newton, M.; Sutin, N. *J. Photochem. Photobiol.* **1994**, *A82*, 47.

(70) Nelsen, S. F.; Newton, M. D. *J. Phys. Chem. A* **2000**, *104*, 10023.
(71) Johnson, R. C.; Hupp, J. T. *J. Am. Chem. Soc.* **2001**, *123*, 2053.

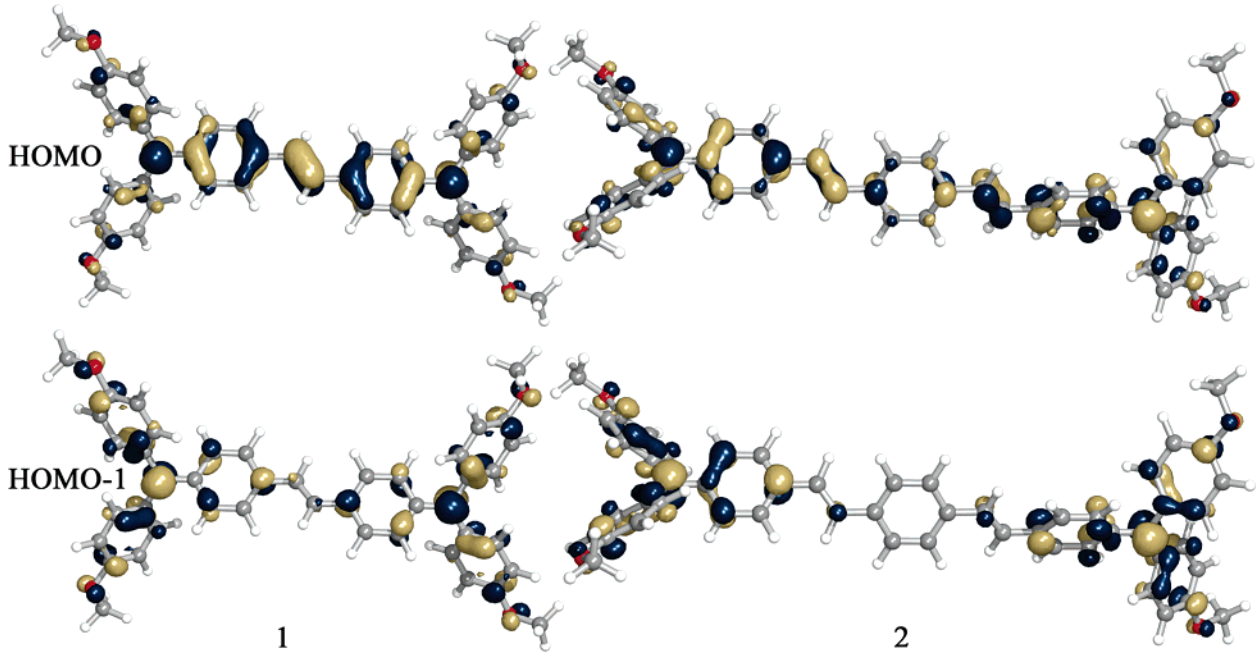

Figure 5. Contour plots of the HOMO and HOMO-1 for **1** and **2** obtained at the AM1 level.

AM-CI calculations[70,71] of the monocation state dipole moments.[72] These values are also given in Table 3; AM1 values of R_{NN} and of the *adiabatic* electron-transfer distance, R_{12} ($\Delta\mu_{12}$/e), are also given. Estimates of the *diabatic* electron-transfer distance, R, from either eq 6 or 7, are considerably smaller than the geometric N−N separations, R_{NN}, reflecting the bridge contributions to the diabatic states (see also Figure 3). In $\mathbf{2}^+$, consistent with its assignment to class-II, the adiabatic and diabatic electron-transfer distances are similar to one another. In the more delocalized $\mathbf{1}^+$, R_{12} is much smaller than R. However, the small nonzero value of R_{12} of this system is more consistent with a species on the class-II/III borderline than a fully delocalized class-III cation. TD-DFT estimates of $\mu_\pm$ give qualitatively similar results (i.e, $R < R_{NN}$) but somewhat smaller values of $\mu_\pm$ and, hence, of R are obtained; we have previously reported a TD-DFT value of $R_{[eq6]}$ for $\mathbf{L1}^+$ to be 6.89 Å.[27]

We calculated values of the electronic coupling, V, for $\mathbf{1}^+$ and $\mathbf{2}^+$ from eq 2 using values of R from Table 3 and experimental values of μ_{ge} and $\bar{\nu}_{max}$ from Table 2. These values are collected in Table 4 and compared with the corresponding values for $\mathbf{L0}^+$, $\mathbf{L0'}^+$, $\mathbf{L1}^+$, and $\mathbf{L2}^+$. The species with double bonds in the bridge clearly show stronger electronic coupling than the analogous triple-bonded species, consistent with previous studies of MV systems with ferrocenyl,[73,74] octahedral Ru,[75] and dimethoxybenzene[14] redox centers.[76] AM1/UHF calculations for bis(dimethylamino)polyene and polyyne cations also predict stronger coupling in the former class.[4] However,

Table 4. Electronic Coupling, V (in cm^{-1}), Calculated According to Equation 2 (μ_{ge}, $\bar{\nu}_{max}$, and R values are taken from Table 3), and According to Equation 5 (for class-III species). All Data Refer to CH_2Cl_2 or, in Parentheses, to CH_2Cl_2/0.1 M $[^nBu_4N]^+[PF_6]^-$

	class assumed	$V_{[eq2]}$			$V_{[eq5]}$
		R_{NN}[a]	$R_{[eq6]}$	$R_{[eq7]}$	
$\mathbf{1}^+$	III	1400	1950	2890	3020 (3140)
$\mathbf{2}^+$	II	700	1140	1510	–
$\mathbf{L0}^+$	III	(3250[b])	–	–	(4765[b])
$\mathbf{L0'}^+$	III	(1550[b])	(1990[d])	–	(3180[b])
$\mathbf{L1}^+$	II	1080 (1200[b])	1500 (1665[d])	–	–
$\mathbf{L2}^+$	II	490[c] (500[b])	–	1000[e]	–

[a] R_{NN} values used for all except $\mathbf{1}^+$ and $\mathbf{2}^+$ were from AM1/UHF optimizations of the cations and are taken from ref 22. [b] μ_{ge} and $\bar{\nu}_{max}$ data taken from ref 22. [c] A value of 540 cm^{-1} is obtained using the μ_{ge} and $\bar{\nu}_{max}$ values from ref 25. [d] μ_{ge} and $\bar{\nu}_{max}$ data taken from ref 22; ZINDO/CIS value of $R_{[eq6]}$ taken from ref 29. [e] From ref 32.

as we have previously noted,[46] $\mathbf{1}^+$ and $\mathbf{L1}^+$ are, to the best of our knowledge, the first case where an alkene/alkyne pair of MV species fall on different sides of the class-II/III borderline. Interestingly, the stilbene-bridged species, $\mathbf{1}^+$, shows very similar coupling to its biphenyl-bridged analogue, $\mathbf{L0'}^+$; presumably, this is due to a canceling resulting from the interplay of opposing effects, perhaps associated with different bridge lengths and planarities. Literature precedents show that such canceling effect is not necessarily expected; in an example with bis(dialkoxybenzene) redox centers, a stilbene-bridged species showed a coupling ca. 1.4 times that of its biphenyl analogue,[14] whereas, in a ruthenium example, a species with a 4,4′-bipyridyl bridge shows a coupling ca. 1.2 times that of a 1,2-bis(4-pyridyl)ethene bridge.[75]

We were also interested in comparing the trends in electronic coupling obtained from various theoretical estimates. Table 5 shows couplings estimated from Koopmans' theorem (KT),[77] that is, from taking half the energy difference between the HOMO and HOMO-1, using various computational techniques.

(72) Experimental values of $\Delta\mu_{12}$ are, in principle, accessible through Stark spectroscopy. Indeed, several studies have focused on the determination of $\Delta\mu_{12}$ for inorganic MV compounds; for example, see: Oh, D. H.; Sano, M.; Boxer, S. G. *J. Am. Chem. Soc.* **1991**, *113*, 6880.
(73) Le Vanda, C.; Bechgaard, K.; Cowan, D. O. *J. Org. Chem.* **1976**, *41*, 2700.
(74) Ribou, A. C.; Launay, J.-P.; Sachtleben, M. L.; Li, H.; Spangler, C. W. *Inorg. Chem.* **1996**, *35*, 3735.
(75) Sutton, J. E.; Taube, H. *Inorg. Chem.* **1981**, *20*, 3125.
(76) Other donor−acceptor interactions have also been found to be more strongly mediated through alkenes; for example, (*E*)-FcCH=CHB(mes)$_2$ {Fc = ferrocenyl, mes = 2,4,6-trimethylphenyl} shows a lower-energy and more intense donor−acceptor CT transition than (*E*)-FcC≡CB(mes)$_2$ (Yuan, Z.; Stringer, G.; Jobe, I. R.; Kreller, D.; Scott, K.; Koch, L.; Taylor, N. J.; Marder, T. B. *J. Organomet. Chem.* **1993**, *452*, 115).
(77) Koopmans, T. *Physica* **1933**, *1*, 104.

Table 5. Estimates of *V* from Koopmans' Theorem, Calculated at Neutral Geometry Using Three Different Methods

	V_{KT}/cm^{-1}		
	AM1	B3LYP/6-31G*	AM1 at B3LYP/6-31G* geometry
$\mathbf{1}^+$	1180	1840	1390
$\mathbf{2}^+$	550	1170	800
$\mathbf{3}^+$	260	720	430
$\mathbf{4}^+$	110	440	230

The couplings according to the KT calculations show similar trends irrespective of the method used; the electronic coupling decreases more-or-less exponentially with R_{NN}. However, the values of the couplings are rather sensitive to the details of the method employed, as we have found before,[27] as, to a lesser extent, are the decay constants. Interestingly, it should be noted that the KT estimates of couplings for $\mathbf{1}^+$ are somewhat lower than those obtained for the alkyne analogue $\mathbf{L1}^+$,[27] in contradiction to the results indicated by the optical data. However, if the KT calculation is carried out using AM1 using the symmetrical DFT cation geometry for $\mathbf{1}^+$, a coupling of 2270 cm^{-1} is obtained, greater than the 1730 cm^{-1} obtained for $\mathbf{L1}^+$ using the symmetric DFT cation geometry.[27] These differences are presumably related to the nonplanar geometry of neutral **1**; greater coupling relative to $\mathbf{L1}^+$ is only calculated when the planarized cation geometry is used. We have previously seen a similar effect, in which using KT at neutral geometry for 4,4′-bis(di-*p*-anisylamino)biphenyl gives a smaller coupling than for $\mathbf{L1}^+$,[27] again in contradiction to optical data; the biphenyl bridge of the former species is also twisted in the neutral molecule and planarized in the cation.[22]

Discussion and Summary

The narrowness, asymmetry, and solvatochromism of the IVCT band of the 4,4′-bis(di-*p*-anisylamino)stilbene MV cation, $\mathbf{1}^+$, indicates that this species falls into a similar régime of delocalization as bis(diarylamino)biphenyl cations. Several recent crystallographic and vibrational studies,[30,44] including one of $\mathbf{1}^+$, indicate that these species characterized by narrow asymmetric IVCT bands do belong to Robin and Day's class III.[46] In contrast, the triple-bonded analogue of $\mathbf{1}^+$, $\mathbf{L1}^+$, appears to belong to class II, consistent with both a previous NIR study[22] and with vibrational data.[46] While there is ample precedent for stronger coupling in double-bonded versus triple-bonded systems, it is interesting that the increased coupling (ca. 30% according to Hush analysis) in the former case is sufficient in this case to place double- and triple-bonded systems into different régimes of delocalization. Since $\mathbf{1}^+$ belongs to class III, we can estimate the coupling both from Hush theory and from setting the coupling to half the IVCT transition energy; comparison of these values indicates that the diabatic electron-transfer distance in $\mathbf{1}^+$ is considerably less than the geometric N−N separation, a result consistent with quantum-chemical estimates of the diabatic electron-transfer distance for $\mathbf{1}^+$ and also for the longer class-II homologues, $\mathbf{2}^+$−$\mathbf{4}^+$. The 1,4-bis-[4-(di-*p*-anisylamino)styryl]benzene cation, $\mathbf{2}^+$, also shows stronger coupling (ca. 40% higher) relative to its triple-bonded analogue, $\mathbf{L2}^+$, although the coupling is sufficiently low that both species belong to class II. AM1 calculations also support the assignment of $\mathbf{1}^+$ and $\mathbf{2}^+$ to classes III and II, respectively.

In $\mathbf{3}^+$, the IVCT overlaps with another band, which we attribute to a bridge-to-cation ($B \rightarrow D^+$) charge transfer, while that of $\mathbf{4}^+$ is sufficiently weak that it cannot be detected under the $B \rightarrow D^+$ band. It is worth noting that the $B \rightarrow D^+$ bands seen in $\mathbf{3}^+$ and $\mathbf{4}^+$ could be easily be mis-assigned as IVCT bands since they occur at rather long wavelength (ca. 1200 nm) and are rather broad and somewhat solvatochromic; only by comparison with the spectra of the corresponding dications or with the mononuclear model compound, $\mathbf{5}^+$, can their origin be clarified.

In general, our experimental and computational data show that the electronic coupling decreases as one moves from $\mathbf{1}^+$ to $\mathbf{4}^+$. The decrease in coupling in the monocations is paralleled by a decrease in the coupling between the two triarylaminium centers in the corresponding dications: $\mathbf{1}^+$ appears to be a class-III species and $\mathbf{1}^{2+}$ is diamagnetic; $\mathbf{4}^+$ has a barely detectable IVCT band and so can be regarded as approaching the class-I limit, while the ESR signal intensity for $\mathbf{4}^{2+}$ is consistent with a system with minimal coupling between two independent $S = {}^1/_2$ centers. Thus, we have mapped the transition from strongly coupled and delocalized to very weakly coupled and rather localized behavior in both mono- and dications of these bis-(diarylamino)phenylenevinylenes as a function of chain length.

Experimental Details

General. Electrochemical measurements were carried out under argon on dry (distilled from CaH_2) deoxygenated dichloromethane solutions ca. 10^{-4} M in analyte and 0.1 M in tetra-*n*-butylammonium hexafluorophosphate using a BAS potentiostat, a glassy carbon working electrode, a platinum auxiliary electrode, and, as a pseudo-reference electrode, a silver wire anodized in 1 M aqueous potassium chloride. Potentials were referenced to ferrocenium/ferrocene by using cobaltocenium hexafluorophosphate[78] as an internal reference (since many of the redox events of interest were at similar potentials to that of ferrocene). Cyclic voltammograms were recorded at a scan rate of 50 mV s^{-1}; differential pulse voltammograms were run at 20 mV s^{-1}, with a pulse height of 50 mV, on the same samples, to afford better resolution of the overlapping peaks in **1** (no additional features were resolved for **2**−**5**). UV−vis−NIR spectra were recorded in 1 cm cells using a Varian Cary 5E spectrometer. Room-temperature ESR spectra were acquired using a Bruker EMX spectrometer. Compound **1** was prepared as described previously,[46] while compounds **L1** and **L2** were prepared by the literature procedures;[22] other chemicals were either obtained commercially or prepared as described below.

(*E*,*E*)-1,4-Bis[4-{bis(4-methoxyphenyl)amino}styryl]benzene, 2. This compound was synthesized in 75% yield from 4-{bis(4-methoxyphenyl)amino}benzaldehyde,[79] essentially as recently described elsewhere,[53] but using tetramethyl 1,4-xylene-α,α′-diyl diphosphonate[80] in place of the tetraethyl phosphonate, running the reaction in THF for 2 h (rather than in DMF overnight) and purifying the product using column chromatography (silica gel, 4:1 hexanes/ethyl acetate). The ^1H NMR spectrum was in agreement with the published data.[53]

(78) We measured the cobaltocenium/cobaltocene couple at −1320 mV versus ferrocenium/ferrocene in dichloromethane; previous studies give values of −1350 mV (Koelle, U.; Khouzami, F., *Angew. Chem., Int. Ed. Engl.* **1980**, *19*, 640), −1330 mV (ref 58), and −1320 mV (Barlow, S. *Inorg. Chem.* **2001**, *40*, 7047).

(79) 4-Bis(4-methoxyphenyl)aminobenzaldehyde has previously be obtained by a variety of syntheses; we obtained it in 79% yield through the Vilsmeier formylation of *N*,*N*-bis(4-methoxyphenyl)-*N*-phenylamine, which was itself obtained using Pd-catalyzed coupling chemistry from bis(4-methoxyphenyl)-amine and bromobenzene.

(80) This compound was synthesized essentially according to the literature (Tewari, R. S.; Kumari, N.; Kendurkar, P. S. *Ind. J. Chem.* **1977**, *15B*, 753), but we did not find it necessary to distill the product after removing excess trimethyl phosphite and dimethyl methylphosphonate under reduced pressure.

***N,N*-Bis(4-methoxyphenyl)-*N*-(4-vinylphenyl)amine, S1.**[81] Potassium *tert*-butoxide (10 mL of a 1.6 M solution in THF) was added to 4-{bis(4-methoxyphenyl)amino}benzaldehyde[79] (2.00 g, 6.00 mmol) and methyl triphenylphosphonium iodide (3.15 g, 7.80 mmol) in THF (50 mL) at room temperature, and the reaction was stirred for 3 h. The mixture was poured into distilled water and extracted into ethyl acetate. The pure compound (1.73 g, 89%) was obtained after silica gel chromatography, eluting with dichloromethane/hexane (1:1). ^{1}H NMR (CD_2Cl_2, 300 MHz): δ 7.23 (d, J = 8.7 Hz, 2H), 7.08 (d, J = 8.7 Hz, 4H), 6.91 (d, J = 8.7 Hz, 2H), 6.85 (d, J = 8.7 Hz, 4H), 6.68 (dd, J = 17.7, 10.8 Hz, 1H), 5.58 (d, J = 17.7 Hz, 1H), 5.10 (d, J = 10.5 Hz, 1H), 3.81 (s, 6H). ^{13}C NMR (CD_2Cl_2, 75 MHz): δ 155.75, 148.32, 140.73, 136.23, 129.83, 126.79, 126.43, 120.35, 114.57, 110.99, 55.35. GC/MS m/z 331 (M^+).

(*E,E,E*)-4,4′-Bis[4-{bis(4-methoxyphenyl)amino}styryl]stilbene, 3. (*E*)-4,4′-dibromostilbene[46,82] (0.77 g, 2.27 mmol) and **S1** (1.50 g, 45.0 mmol) were dissolved in DMF (10 mL) under nitrogen, and tri-*o*-tolylphosphine (0.05 g, 0.16 mmol), triethylamine (3 mL), and palladium(II) acetate (0.02 mg, 0.09 mmol) were added. The reaction mixture was heated to 90 °C for 24 h. After the mixture was cooled to room temperature, it was poured into ethanol. The precipitate formed was collected on a filter and washed thoroughly with ethanol. The crude product was purified by column chromatography, eluting with hexane/ethyl acetate (8:1), to afford an orange solid (1.70 g, 89%). ^{1}H NMR (CD_2Cl_2, 500 MHz): δ 7.55 (d, J = 9.0 Hz, 4H), 7.52 (d, J = 8.5 Hz, 4H), 7.38 (d, J = 8.5 Hz, 4H), 7.17 (s, 2H), 7.12 (d, J = 16.0 Hz, 2H), 7.11 (d, J = 9.0 Hz, 8H), 7.00 (d, J = 16.0 Hz, 2H), 6.92 (d, J = 8.5 Hz, 4H), 6.89 (d, J = 9.0 Hz, 8H), 3.78 (s, 12H). ^{13}C NMR (CD_2Cl_2, 125 MHz): δ 156.57, 148.87, 140.93, 137.60, 136.57, 129.68, 128.58, 128.15, 127.54, 127.16, 127.12, 126.81, 125.66, 120.38, 115.03, 55.80. HRMS (EI) calcd for $C_{58}H_{50}N_2O_4$: 838.3771. Found: 838.3736. Anal. Calcd for $C_{58}H_{50}N_2O_4$: C, 83.03; H, 6.01; N, 3.34. Found: C, 83.38; H, 6.03; N, 3.00.

(*E,E*)-1,4-Bis(4-bromostyryl)benzene, S2.[83] Potassium *tert*-butoxide (2.0 g, 16 mmol) was added to a solution of 4-bromobenzaldehyde (2.46 g, 13.0 mmol) and tetraethyl 1,4-xylene-α,α′-diyl diphosphonate (2.00 g, 5.00 mmol) in THF (30 mL) over 2 h, during which time the product precipitated out as a yellow solid. The mixture was stirred at room temperature for an additional 1 h. The solid was filtered and washed several times with ethanol. The yield of product was 2.90 g (50% assuming it to be pure material). This compound was used in the next reaction without further characterization due to low solubility.

(*E,E,E,E*)-1,4-Bis(4-[4-{bis(4-methoxyphenyl)amino}styryl]styryl)-benzene, 4. This compound was prepared in the same way as **3** from **S2** (0.44 g, 1.00 mmol assuming pure material), **S1** (0.70 g, 2.00 mmol), tri-*o*-tolylphosphine (0.025 g, 0.082 mmol), triethylamine (2 mL), and palladium(II) acetate (0.01 g, 0.045 mmol). The crude product was purified by column chromatography, eluting with dichloromethane, to afford an orange solid (0.78 g, 41%). ^{1}H NMR ($CDCl_3$, 300 MHz): δ 7.49 (s, 4H), 7.46 (s, 8H), 7.31 (d, J = 8.1 Hz, 4H), 7.10 (s, 4H), 7.05 (d, J = 9.3 Hz, 8H), 7.02 (d, J = 16.2 Hz, 2H), 6.92 (d, J = 16.2 Hz, 2H), 6.89 (d, J = 9.0 Hz, 4H), 6.83 (d, J = 9.0 Hz, 8H), 3.79 (s, 12H). ^{13}C NMR (CD_2Cl_2, 125 MHz): δ 156.61, 140.92, 137.72, 137.17, 136.53, 128.66, 128.52, 128.08, 127.57, 127.20, 126.84, 125.66, 120.39, 115.05 (the compound is poorly soluble, and we were unable to observe the remaining four expected aromatic/vinylic ^{13}C peaks), 55.83. HRMS (EI) calcd for $C_{66}H_{56}N_2O_4$: 940.4240. Found: 940.4241. Anal. Calcd for $C_{66}H_{56}N_2O_4$: C, 84.23; H, 6.00; N, 2.98. Found: C, 83.91; H, 6.17; N, 3.05.

(*E*)-4-Bromo-4′-*tert*-butylstilbene, S3. To a solution of 4-*tert*-butylbenzaldehyde (1.1 g, 6.8 mmol) and diethyl 4-bromobenzylphosphonate (2.0 g, 6.8 mmol) in THF (40 mL) was added potassium *tert*-butoxide (1.3 g, 13.6 mmol) at room temperature; the reaction was stirred for 2 h. The mixture was then poured into water and extracted by ethyl acetate. After removing the solvent under vacuum, the crude product was purified by crystallization from methanol. The yield of product was 1.70 g (79%). ^{1}H NMR ($CDCl_3$, 300 MHz): δ 7.45 (d, J = 8.1 Hz, 2H), 7.43 (d, J = 7.8 Hz, 2H), 7.56 (d, J = 8.7 Hz, 2H), 7.35 (d, J = 8.4 Hz, 2H), 7.07 (d, J = 16.2 Hz, 1H), 6.97 (d, J = 16.2 Hz, 1H), 1.32 (s, 9H). ^{13}C NMR ($CDCl_3$, 75 MHz): δ 151.32, 136.36, 134.06, 131.61, 129.11, 127.77, 126.51, 126.20, 125.59, 120.96, 34.72, 31.34. GC/MS m/z 314 (M^+). Anal. Calcd for $C_{18}H_{19}Br$: C, 68.58; H, 6.07. Found: C, 68.39; H, 6.18.

(*E*)-4-Formyl-4′-*tert*-butylstilbene, S4. To a solution of **S3** (2.0 g, 6.3 mmol) in dry THF (40 mL) was added *n*-butyllithium (4 mL of a 2.5 M solution in hexane, 10.0 mmol) and stirred at −78 °C for 30 min. DMF (0.7 g, 10 mmol) was then added dropwise at −78 °C, and the reaction was stirred for 2 h at room temperature. The resulting solution was poured into water (50 mL) and extracted with ethyl acetate. After removing the solvent under vacuum, the crude product was purified by column chromatography, eluting with hexane, to give 1.0 g (60%) of a pale yellow powder. ^{1}H NMR ($CDCl_3$, 300 MHz): δ 9.97 (s, 1H), 7.84 (d, J = 8.1 Hz, 2H), 7.63 (d, J = 7.2 Hz, 2H), 7.48 (d, J = 8.4 Hz, 2H), 7.40 (d, J = 8.1 Hz, 2H), 7.24 (d, J = 16.2 Hz, 1H), 7.09 (d, J = 16.2 Hz, 1H), 1.32 (s, 9H). ^{13}C NMR ($CDCl_3$, 75 MHz): δ 191.46, 151.68, 143.54, 134.99, 133.63, 131.93, 130.13, 126.56, 125.85, 125.45, 115.51, 34.79, 31.31. GC/MS m/z 264 (M^+). Anal. Calcd for $C_{19}H_{20}O$: C, 86.32; H, 7.63. Found: C, 86.47; H, 7.55.

(*E,E*)-1-(4-Bromostyryl)-4-(4-*tert*-butylstyryl)benzene, S5. To a solution of **S4** (1.0 g, 3.8 mmol) and diethyl 4-bromobenzylphosphonate (1.3 g, 4.5 mmol) in THF (30 mL) was added potassium *tert*-butoxide (0.73 g, 7.6 mmol) at room temperature and stirred for 2 h. The mixture was poured into methanol and filtered, and then washed with methanol. The crude product was purified by crystallization from hot methanol to give 1.0 g (63%) of a pale yellow powder. ^{1}H NMR (CD_2Cl_2, 500 MHz): δ 7.54 (s, 4H), 7.49 (app. d, app. J = 7.5 Hz, 4H), 7.42 (m, 4H), 7.15 (m, 4H), 1.38 (s, 9H). ^{13}C NMR (CD_2Cl_2, 125 MHz): δ 151.34, 137.65, 136.74, 136.50, 134.91, 132.24, 129.46, 129.04, 128.36, 127.82, 127.53, 127.29, 127.20, 126.69, 126.07, 121.69, 35.06 31.70. HRMS (EI) calcd for $C_{26}H_{25}Br$: 416.1140. Found: 416.1132. Anal. Calcd for $C_{26}H_{25}Br$: C, 74.82; H, 6.04. Found: C, 74.77; H, 6.11.

(*E,E,E*)-1-{Bis(4-methoxyphenyl)amino}-4-[4-{4-(4-*tert*-butylstyryl)-styryl}styryl]benzene, 5. S5 (0.20 g, 0.55 mmol) and **S1** (0.18 g, 0.55 mmol) were dissolved in DMF (20 mL) under nitrogen, and tri-*o*-tolylphosphine (2 mg, 0.065 mmol), triethylamine (1 mL), and palladium(II) acetate (1.00 mg, 0.044 mmol) were added. The reaction mixture was heated to 110 °C for 24 h. After the mixture was cooled to room temperature, it was poured into methanol. The precipitate formed was collected on a filter and washed thoroughly with ethanol. The crude product was purified by column chromatography on silica gel, eluting with hexane and dichloromethane (10/1), to give 0.17 g (45%) as a yellow powder. ^{1}H NMR (CD_2Cl_2, 500 MHz): δ 7.57 (s, 4H), 7.55 (d, J = 7.0 Hz, 2H), 7.52 (d, J = 8.5 Hz, 2H), 7.44 (d, J = 8.0 Hz, 2H), 7.39 (d, J = 9.0 Hz, 2H), 7.19 (s, 2H), 7.16 (d, J = 9.5 Hz, 2H), 7.20−7.10 (m, 3H), 7.11 (d, J = 8.5 Hz, 4H), 7.02 (d, J = 16.2 Hz, 1H), 6.91 (d, J = 8.7 Hz, 2H), 6.89 (d, J = 7.0 Hz, 4H), 3.84 (s, 6H), 1.33 (s, 9H). ^{13}C NMR (CD_2Cl_2, 125 MHz): δ 156.61, 151.37, 148.82, 140.95, 137.70, 137.28, 137.02, 136.55, 134.89, 128.69, 128.61, 128.43, 128.11, 127.68, 127.56, 127.20, 127.15, 127.10, 126.83, 126.56, 126.05, 125.66, 120.39, 115.06 (the remaining two expected aromatic/vinylic ^{13}C peaks not observed, presumably due to overlap), 55.83, 34.92, 31.40. MS (EI) m/z 667 ([M]$^+$, 100%), 652 ([M − CH_3]$^+$, 15%), 637 ([M − $2CH_3$]$^+$, 13%), 565 (10%). Anal. Calcd for $C_{48}H_{45}NO_2$: C, 86.32; H, 6.79; N, 2.10. Found: C, 85.96; H, 6.89; N, 1.86.

Chemical Oxidation of 1−5, L1, and L2. Monocations and dications of the bis(triarylamine) species and $\mathbf{5}^+$ were generated in solution by addition of appropriate amounts of tris(4-bromophenyl)-aminium hexafluoroantimonate (Aldrich) in dry solvents (<0.1 equiv for monocations, 2 equiv for dications). Monocations were generated

(81) Ferrar, W. T.; Jin, X.; Sorriero, L. J.; Weiss, D. S. Eur. Patent Application, 2004.
(82) Baumgarten, M.; Yuksel, T. *Phys. Chem. Chem. Phys.* **1999**, *1*, 1699.

by addition of $[(4\text{-}BrC_6H_4)_3N]^+[SbCl_6]^-$ to large excesses of the neutral species; absorptivities were calculated assuming all of the oxidizing agent added results in formation of monocation and that disproportionation is negligible at these concentration ratios. Consistent with these assumptions, we do not observe unreacted oxidizing agent in the optical spectra, nor do we see evidence for disproportionation for $\mathbf{1}^+$ and $\mathbf{2}^+$, where the dication absorbs at very different energy to the monocation. In the case of $\mathbf{3}^+$ and $\mathbf{4}^+$, where mono- and dication spectra are closely overlapping, we established that we were in a régime of negligible disproportionation by showing that the spectra obtained were independent of the exact ratio of oxidizing agent to neutral molecule used. Dications were generated by addition of 2 equiv of $[(4\text{-}BrC_6H_4)_3N]^+[SbCl_6]^-$ to the neutral species, and the electron-transfer reaction was again assumed to be complete in calculating absorptivities. Neither the side product, $(4\text{-}BrC_6H_4)_3N$, nor neutral **1**−**5** absorb in the energy range plotted in Figure 2. Optical and ESR spectra for $\mathbf{1}^{2+}$ were also recorded using the isolated bis(hexafluoroantimonate) salt described elsewhere.[60]

Computational Methods. Geometry optimizations for neutral molecules were performed using both the semiempirical Hartree−Fock Austin Model 1 (AM1) and Density Functional Theory (DFT) methods. The DFT calculations were carried out using the B3LYP functional, in which Becke's three-parameter hybrid exchange functional is combined with the Lee−Yang−Parr correlation functional,[84−86] with a 6-31G* split valence plus polarization basis set. Correlated semiempirical AM1/CI and AM1-UHF methods were utilized for the investigations of the radical cations. While AM1-UHF predicts asymmetric geometries for each of the molecular systems investigated, the technique suffered from high degrees of spin contamination ($\langle S_2 \rangle \sim 5$). Therefore, only the AM1/CI results are reported. The configuration−interaction (CI) space for the coupled AM1/CI method was restricted to the orbitals corresponding to the HOMO-1 and HOMO in the neutral species for each molecular system. In addition, UB3LYP/6-31G* was used for optimization of the geometry of $\mathbf{1}^+$.

Excitation energies and transition dipole moments for $\mathbf{1}^+$−$\mathbf{4}^+$ were calculated with the correlated semiempirical Zerner's intermediate neglect of differential overlap (ZINDO/CIS) method.[87] The calculations were executed using the radical cation electronic configuration with the neutral geometry obtained from AM1. The use of the optimized radical cation geometries led to large degrees of spin contamination and, hence, unreliable results. All AM1-based methods were carried out using the implementation in the AMPAC[88] software package, while the DFT and ZINDO calculations were performed with Gaussian98.[89]

Acknowledgment. This material is based upon work supported in part by the STC Program of the National Science Foundation under Agreement Number DMR-0120967 and by the NSF Grant CHE-0342321.

Supporting Information Available: Calculated geometric parameters for **1**−**4** and $\mathbf{1}^+$−$\mathbf{4}^+$; full atomic coordinates and absolute energies for computed geometries; complete citations for refs 44, 46, 60, and 89. This material is available free of charge via the Internet at http://pubs.acs.org.

JA054136E

(83) Hu, Q.-S.; Vitharana, D.; Liu, G.-Y.; Jain, V.; Wagaman, M. W.; Zhang, L.; Lee, T. R.; Pu, L. *Macromolecules* **1996**, *29*, 1082.
(84) Becke, A. D. *Phys. Rev.* **1988**, *A38*, 3098.
(85) Becke, A. D. *J. Chem. Phys.* **1993**, *98*, 5648.
(86) Lee, C. T.; Yang, W. T.; Parr, R. G. *Phys. Rev.* **1988**, *B37*, 785.
(87) Zerner, M. C.; Loew, G. H.; Kichner, R. F.; Mueller-Westerhoff, U. T. *J. Am. Chem. Soc.* **1980**, *102*, 589.
(88) *AMPAC 6.55 User's Manual*; Semichem: 7128 Summit, Shawnee, KS 66216, 1997.
(89) Frisch, M. J. et al. *Gaussian 98*; Gaussian Inc.: Pittsburgh, PA, 1995.